Computational Materials Science 74 (2013) 12–16

Contents lists available at SciVerse ScienceDirect

Computational Materials Science

journal homepage: www.elsevier.com/locate/commatsci

Vibrations induced by different charged oxygen vacancies in quartz-like GeO_2

A.N. Kislov *, A.F. Zatsepin

Ural Federal University, 19 Mira St., Ekaterinburg 620002, Russia

ARTICLE INFO

Article history:
Received 20 April 2012
Received in revised form 6 March 2013
Accepted 8 March 2013
Available online 9 April 2013

Keywords:
α-Quartz
Oxygen vacancies
Defect structure
Localized vibrations

ABSTRACT

We have studied local configurations and vibrations of oxygen vacancies in different charged states in α-quartz GeO_2 by computer simulation. First-principles potential of the Buckingham type has been used in calculations. The investigation of the lattice dynamics in defective crystal is performed using the phonon local density of states. The calculation of the densities of states is facilitated with Lanczos recursion. Frequencies of localized vibrations induced by oxygen vacancies are determined.

1. Introduction

The progress in development of micro- and optoelectronics demands the investigation of promising materials. Due to unique combination of physical properties, germanium dioxide is compound with a variety of technological applications. However this material has not been the subject of extensive studies unlike silicon dioxide. At ambient pressure there are three solid GeO_2 modifications: a rutile tetragonal structure, an α-quartz trigonal structure and an amorphous glass [1]. The crystal structure and properties of GeO_2 with the α-quartz-type ideal structure have been studied both experimentally [2–8] and theoretically [9–13]. The calculations of the geometric structure and the physical properties are also known for perfect and defective rutile-type GeO_2 phase [14,15]. Many of the peculiar characteristics of GeO_2 are determined by the presence of point defects and are connected with dynamic processes occurring with participation of defects.

The correct description of these processes requires information about localized vibrations induced by defects. In many cases this information can be obtained only from numerical simulations. An important class of intrinsic defects in germanium dioxide is related to oxygen vacancies that may exist in different charged states. One can distinguish several types of such defects. In particular, neutral vacancies V^0 are the variant of so-called oxygen-deficiency centers (ODCs) forming the main luminescent properties of GeO_2 modifications [16,17]. Positively single-charged vacancies V^{+1} correspond to well-known paramagnetic E′-type centers that are the most studied defects [18]. In addition it is assumed that there are doubly positively charged vacancies V^{+2}, although these centers are not found experimentally.

We reported earlier [19] the results of model calculations of the local lattice dynamics of α-quartz SiO_2 containing O-vacancies in different charged states. At the same time the lattice dynamics of α-quartz-like GeO_2 with oxygen vacancies has not been analyzed so far. The effect of O-vacancies on the vibration spectrum is still not well understood.

In the present work we are considering vibrational properties of quartz-like GeO_2 with oxygen vacancies in three states: V^{+2}, V^{+1} and V^0. The influence of these vacancies on the structure and the phonon spectrum of α-GeO_2 is studied using the numerical modeling.

2. Computer simulation

It is known that the α-quartz lattice of GeO_2 is described by the space group $P3_121$ or $P3_221$. A primitive cell includes three formula units and a hexagonal elementary cell consists of three corner-linked GeO_4 tetrahedra that are connected through a common oxygen atom. Each Ge atom sits at the center of GeO_4 tetrahedron and is surrounded by four oxygen atoms. The GeO_4 tetrahedron is distorted: there are two slightly differing Ge–O distances. Each Ge atom has four nearest-neighbor Ge atoms which are at equal distances. The unit cell can be completely defined by the lattice constants a, c and four internal parameters u, x, y, z as in [20].

Germanium dioxides have ionic–covalent chemical bonds. The computer simulation both of atomic configurations and lattice

* Corresponding author. Tel.: +7 3433754403.
E-mail address: a.n.kislov@ustu.ru (A.N. Kislov).

0927-0256/$ - see front matter © 2013 Elsevier B.V. All rights reserved.
http://dx.doi.org/10.1016/j.commatsci.2013.03.024

dynamics in such crystals containing charged defects encounters considerable difficulties. It is necessary to consider defect-induced relaxation of the surrounding lattice in a large region. Therefore, investigations on static and dynamic behaviors of atoms require the use of a big atomic cluster. The cluster technique allows accurate description of long-range electrostatic interactions. We have already applied it earlier successfully [21,22].

In this approach, the crystal with a defect is divided into several spherical regions: an inner region 1 and an outer region 2 + 3, as shown in Fig. 1. The region 1 is surrounded by the finite region 2. These regions are treated atomistically. The region 3 is represented in the approximation of continuum. Atom displacements in region 1 can be determined by direct minimization of the static lattice energy in the context of the method [23]. Atoms in the region 2 are kept fixed in their ideal positions. Such procedure provides correct calculations of slowly decreasing Coulomb interactions inside the region 1.

The force F_i that acts on the ith atom is obtained using the differentiation of the potential energy $U(r_1, r_2, \ldots, r_N)$ with respect to the relevant coordinates of the atom:

$$F_i = -\frac{\partial U(r_1, r_2, \ldots, r_N)}{\partial r_i}. \quad (1)$$

In our case, the potential energy of the atomic cluster is represented as the sum of pairwise interactions:

$$U(r_1, r_2, \ldots, r_N) = \sum_{k>i}^{N}\sum_{i=1}^{N-1} U_{ik} = \frac{1}{2}\sum_{k\neq i}^{N}\sum_{i=1}^{N} U_{ik}. \quad (2)$$

The interatomic potential U_{ik} is a function of the positions of i and k atoms. It has a specific functional form. We use the ion–ion interaction model [24]

$$U_{ik} = U(r_{ik}) = A_{ik}\exp(-r_{ik}/\rho_{ik}) - \frac{C_{ik}}{r_{ik}^6} + \frac{Z_i Z_k}{r_{ik}}, \quad (3)$$

where the terms describe repulsion, van der Waals and Coulomb interactions, respectively. Here $r_{ik} = |r_k - r_i|$ is the distance between ions i and k; Z_i is the partial charge of the ion i; A_{ik}, ρ_{ik} and C_{ik} are the parameters. The numerical values of parameters appeared in Eq. (3) can be fitted with respect to experimental data [9,10,25] or to the energies obtained from a quantum mechanical calculation [26]. In our calculations, the parameters are used which have been presented in [26]. The choice of these parameters is motivated by the following facts. On one hand, the calculations have reproduced well both the structural and various properties of the perfect crystal including vibrational spectra. On the other hand, parameters of the potential U_{ik} derived from ab initio calculations.

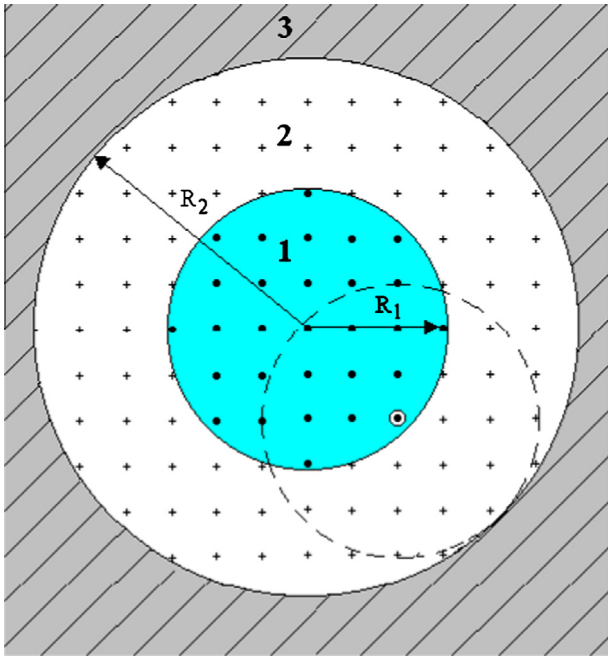

Fig. 1. The structural model of the crystal.

The effect of oxygen vacancies on the vibration spectrum of α-GeO_2 was analyzed by calculating the local densities of states (LDOSs) of phonons in ideal and defective crystals using the Lanczos recursion [27,28]. The Lanczos algorithm is a technique to transform a dynamic matrix of the atomic cluster into an equivalent tridiagonal form.

3. Results

Using the ab initio pair interatomic potentials for α-GeO_2 mentioned above, we modeled the equilibrium structure of a perfect crystal. The obtained values of the lattice constants a, c and unit cell volume Ω are $a = 5.114$ (4.986) Å, $c = 5.736$ (5.647) Å and $\Omega = 129.96$ (121.57) Å^3, where the numbers in parentheses are the experimental values [5] at 300 K. The experimental values are found to be slightly small, but fairly close to those obtained from our calculations.

The simulated Ge–O bond lengths are 1.743 Å for two oxygen ions (denoted by O(1), see Fig. 2) and 1.751 Å for the other two (denoted by O(2)). Each oxygen ion forms only two O–Ge bonds of different lengths. The Ge ion, which is 1.743 Å away from oxygen that can be removed to form a defect, will be designated Ge(1). The Ge ion is labeled Ge(2) when the O–Ge bond is 1.751 Å long. These results are in qualitative agreement with the experimental findings of the work [5], although the bond lengths are slightly larger than the corresponding experimental values: $d_{Ge-O(1)} = 1.737$ Å and $d_{Ge-O(2)} = 1.742$ Å. It should be noted that the authors of work [29] used the same interaction pair potential [26] in molecular dynamics simulations for quartz-like GeO_2. They have obtained the Ge–O bond lengths that are almost identical to our results. Thus, calculations [29] and experimental data [5] can be considered as additional arguments in favor of the correctness of the approach used in present paper.

We also calculated the phonon dispersion curves in highly symmetric directions ([100], [010] and [001]) of the Brillouin zone and the one-phonon density of states (DOS) for perfect α-quartz GeO_2. The phonon DOS was determined by solving the Fourier transform of the dynamic matrix (dimensionality 27×27) for 8500 randomly selected wave vectors of the Brillouin zone. The discrete frequencies were sorted into a histogram of 100 bars. The calculation results are shown in Fig. 3. There are three frequency bands for DOS: an upper limit of the low-frequency band at 10.2 THz, a medium-frequency band between 12.9 and 16.0 THz and a high-frequency band between 26.1 and 28.5 THz. The bands agree very well with the previous computations [26] and with experiments [6]. Experimentally three bands are found: the low-frequency continuum extends to 10.0 THz, the mid-frequency continuum ranges from 12.9 to 17.6 THz, the continuum at high frequency from 25.5 to 28.8 THz.

Then the phonon DOS was calculated using the Lanczos recursion (Fig. 3), in order to test the validity of this method. An analysis of Fig. 3 shows that the $G(\nu)$ curves, which were obtained by different methods, are similar. We have found that a cluster with inner region 1 radius of 19.12 Å containing 2000 ions and with region 2 radius of 25.19 Å containing 4628 ions in which the Lanczos technique is used to 10–12 levels of recursion is sufficient to reproduce phonon LDOS. The upper boundary of the low-frequency band is

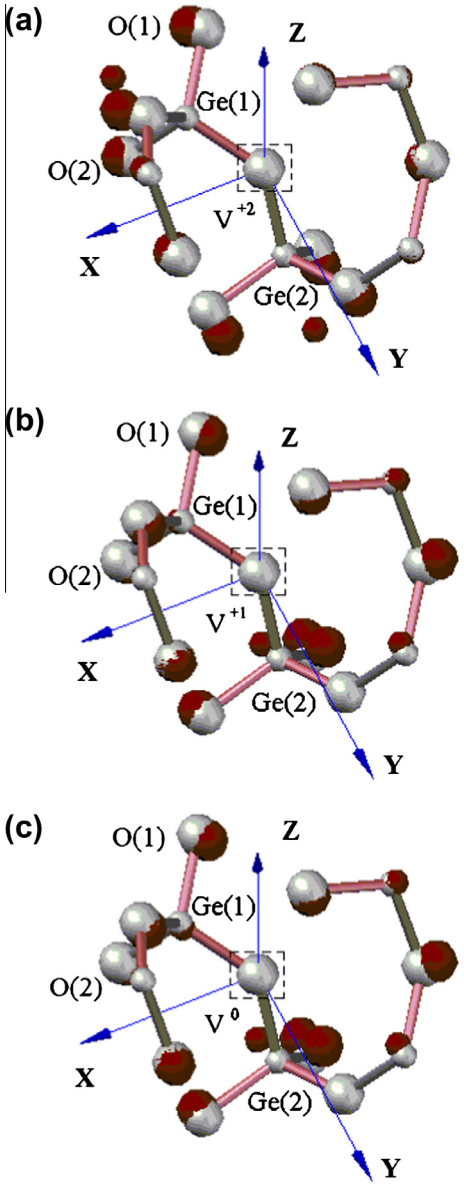

Fig. 2. The structural fragments of α-quartz GeO_2 without defects and with oxygen vacancies: V^{+2} (a), V^{+1} (b), V^0 (c). The ion marked with a square is removed to form an O vacancy. Gray (light) circles indicate the ions before the lattice relaxation, red (dark) circles – after the relaxation. (For interpretation of the references to color in this figure legend, the reader is referred to the web version of this article.)

9.6 THz, the medium-frequency band is between 12.9 and 15.9 THz, the high-frequency band is between 26.1 and 28.5 THz.

Oxygen vacancies V^0, V^{+1} and V^{+2} were described in terms of an ionic approach. The ionic positions around the vacancies have been fully relaxed. These relaxed configurations are shown in Fig. 2. Distortions of the crystal lattice were determined by the potential energy minimization of vacancy-containing α-GeO_2. The values of Ge(1)–Ge(2) distances and also distances between vacancy positions and some ions (O, Ge) in the relaxed configurations are reported in Table 1.

We have calculated the phonon LDOS for all the ions located within a sphere of 3.0 Å radius around oxygen vacancies (V^0, V^{+1} and V^{+2}) or the oxygen ion that removed to form the vacancy. Specific features of the LDOS in a defective crystal, which differ from those of the LDOS in a perfect crystal, corresponded both to resonant vibrations and gap vibrations induced by vacancies. For example, phonon LDOS projected on the Ge(2)-ion displacements in perfect α-GeO_2 and in α-GeO_2 with vacancies are presented in

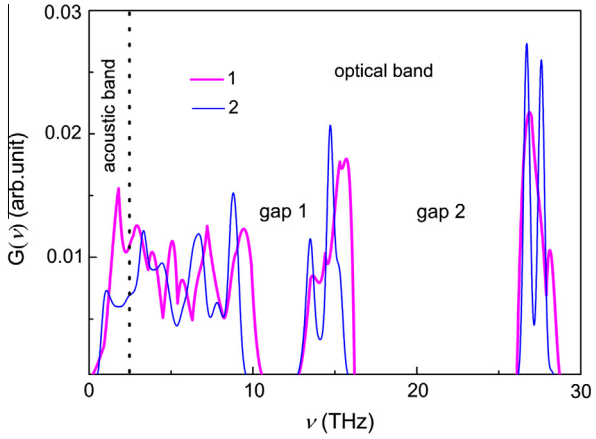

Fig. 3. Phonon DOS of α-quartz GeO_2: calculations using randomly chosen point of the Brillouin zone (curve 1), by a recursive method (curve 2).

Table 1
Distances (Å) between some ions and oxygen vacancies.

V (ion)–ion	Vacancy charge		
	+2	+1	0
V–Ge(1)	3.302	1.781	1.662
V–Ge(2)	3.310	1.494	1.378
V–O(1)	3.040	2.761	2.715
V–O(2)	2.866	2.732	2.724
Ge(1)–Ge(2)	6.106	2.856	2.606

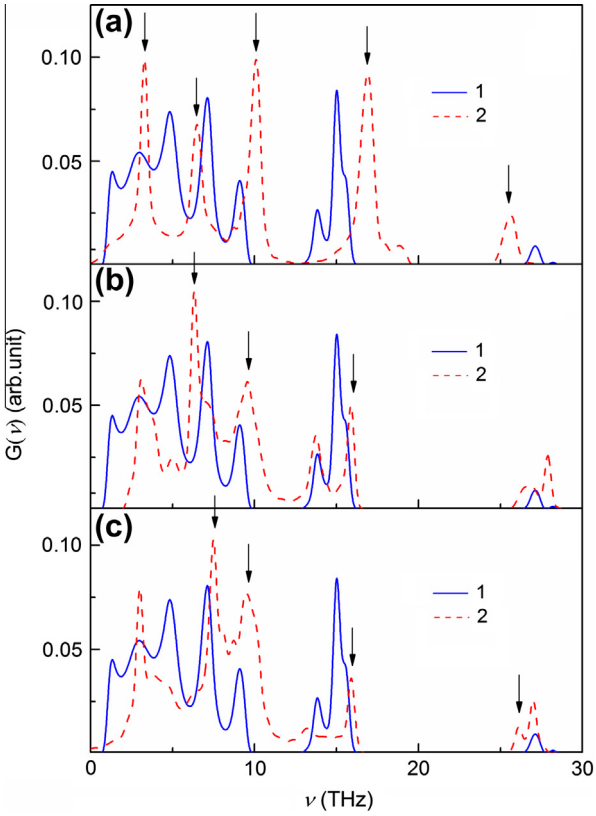

Fig. 4. Phonon LDOS at the site of Ge(2) in perfect α-GeO_2 (curve 1) and in α-GeO_2 with vacancies (curve 2): V^{+2} (a), V^{+1} (b) and V^0 (c). Arrows mark the localized vibrations that involve Ge(2).

Table 2
Frequencies (THz) of resonant (R) and gap (G) vibrations induced by vacancies on nearest ions.

V	Ion	*R*	*G*
V^{+2}	Ge(1)	3.9, 7.2	10.2, 10.8, 20.1, 25.3
	Ge(2)	3.0, 6.3	10.2, 16.5, 25.3
	O(1)	7.2	10.2, 18.6, 23.1, 25.3
	O(2)	4.4, 7.2	10.2, 20.1, 21.0, 23.1, 25.3
V^{+1}	Ge(1)	3.0, 5.1, 8.1, 27.3	12.9, 15.9
	Ge(2)	6.0	9.6, 15.9
	O(1)	5.1, 8.1	15.9
	O(2)	8.1, 27.3	12.9, 15.9
V^{0}	Ge(1)	3.0, 4.8, 8.4	12.9, 15.9, 26.1
	Ge(2)	7.5	9.9, 15.9, 26.1
	O(1)	4.8, 7.5	9.9, 12.9, 15.9, 26.1
	O(2)	8.4, 27.0	9.9, 15.9, 26.1

Fig. 4. The frequencies of localized vibrations in quartz GeO_2 induced by vacancies in different charged states are listed in Table 2.

4. Discussion

We have focused our attention on the structural and vibrational properties of α-quartz GeO_2 with O-vacancies in different charged states. The calculations allowed to perform a comprehensive analysis of the lattice relaxation around oxygen vacancies in different charged states and to show that these defects induce very strong and anisotropic lattice distortions which extend further than about 10 Å from the vacant site. Our results clearly demonstrate that the character of the lattice relaxation strongly depends on the charge state of the oxygen vacancy.

The positively charged vacancy V^{+2} is created by removing an oxygen ion from α-GeO_2. At the same time, the ions surrounding the vacancy V^{+2} are displaced to new equilibrium positions. We have found possible configuration of V^{+2}-centre, which is characterized by different positions of Ge with respect to the vacancy, see Fig. 2a.

The Ge(1) ion adjacent to the oxygen vacancy moves through the plane of the nearest three neighboring oxygen ions and forms the back bond with oxygen. The Ge(2) ion is also shifted from the vacancy and forms the back bond with O. The Ge–Ge distance in the vacancy site is 6.106 Å and it is much larger than the equilibrium distance of 3.223 Å between two Ge in a perfect lattice. The weak Ge(1)–Ge(2) bond brakes. The character of the lattice distortions near V^{+2} vacancy correlates with the fact that this defect has an excessive positive charge with respect to the lattice.

An electron can be localized in the V^{+2} vacancy site. This process is one of the ways of creating a positively charged oxygen vacancy V^{+1}. We assume that the excessive electron density is localized mainly on the O vacancy. According to our calculations, the Ge(2) ion is shifted to the Ge(1) ion. The Ge(1) ion is moved and fixed in an almost planar configuration with three O ions. This relaxed configuration is shown in Fig. 2b. The distance between two Ge ions decreases to 2.856 Å.

When an electron is trapped on a vacancy V^{+1}, the neutral vacancy V^{0} is formed. The calculations predict a displacement of two Ge ions to each other, see Fig. 2c. The Ge(1)–Ge(2) bond strengthens and the bond length between these Ge becomes 2.606 Å. The calculated length of Ge–Ge bond across an oxygen vacancy V^{0} is much shorter than Ge–Ge distance between two nearest Ge in a perfect lattice.

The calculations of the phonon LDOS for the perfect α-GeO_2 demonstrated that vibrations of germanium ions form mainly low- and medium-frequency bands, and vibrations of oxygen ions participate in formation of all three bands of phonon spectrum. The formation of oxygen vacancies in a perfect lattice is accompanied by changes in the phonon DOS. As to the effect of vacancies on the vibrational motion of the ions, it is advisable to analyze it on the example of the Ge(2) ion, the equilibrium position of which is much strongly dependent on the vacancy charge (see Fig. 2). In Fig. 4a it is seen that in the presence of vacancy V^{+2} the low- and middle bands of the phonon LDOS are shifted to the high-frequency part of the spectrum, and high-frequency band is shifted to the low-frequency part. As a result two resonant vibrations with the frequencies of 3.0 and 6.3 THz and also three gap vibrations with the frequencies of 10.2, 16.5 and 25.3 THz appear (see Table 2). It should be noted that not only Ge(2) ion but also Ge(1), O(1) and O(2) ions contribute to the formation of gap vibrations 10.2 and 25.3 THz.

Single-charged oxygen vacancy V^{+1} changes the shape of the phonon LDOS to a lesser extent than double-charged vacancy V^{+2}, see Fig. 4b. In this case the redistribution of the density of states is observed only in low- and middle-frequency bands. V^{+1} induces on the Ge(2) ion only one resonant vibration 6.0 THz and two gap vibrations 9.6 and 15.9 THz. One of the gap vibrations has the frequency which is close to the upper-frequency boundary of the middle-frequency band while the frequency of other vibration is near the low-frequency border of the first forbidden band. In Table 2 one can see that gap vibration with the frequency of 9.6 THz is due to movement of only Ge(2), and the gap vibration 15.9 THz is associated with the movement of Ge(1), O(1) and O(2) ions.

The introduction of a neutral oxygen vacancy V^{0} to the lattice also leads to a redistribution of the phonon density of states, see Fig. 4c. The neutral vacancy induces on Ge(2) ion the resonant vibration with the frequency of 7.5 THz and three gap vibrations with the frequencies of 9.9, 15.9 and 26.1 THz. High-frequency gap vibration 26.1 THz is due to the contribution of the movement both Ge(2) and Ge(1), O(1), O(2) ions.

Thus, the number of the localized vibrations induced by O-vacancies and the values of their frequencies depend on the charged state of defect. At the same time it is necessary to emphasize that the gap vibrations involving the movement of Ge and O ions exist for all types of the oxygen vacancies.

5. Conclusion

In this work we have performed atomistic modeling of quartz-like GeO_2 matrix with O-vacancies in different charged states. The effect of oxygen vacancies on the vibration spectrum was also studied using first-principle potentials of the Buckingham type. The results of the numerical calculations have allowed to evaluate the influence of oxygen vacancies on the structure and the phonon spectrum of α-GeO_2. The values of frequencies of localized vibrations induced by differently charged vacancies were determined.

The data presented above show that the structural and vibrational properties of α-GeO_2 depend substantially on the charge state of the defect. Although our results have predictive character, they can be useful also for interpretation of experimental data, in particular, for the analysis of spectroscopic properties of GeO_2-based materials and regularities of thermal behavior of oxygen-deficient defects such as ODCs and E′-centers.

Acknowledgment

This study was supported by the Russian Foundation for Basic Research (Project No. 13-08-00568).

References

[1] M. Micoulaut, L. Cormier, G.S. Henderson, J. Phys.: Condens. Matter 18 (2006) R753–R784.
[2] G.S. Smith, P.B. Isaacs, Acta Crystallogr. 17 (1964) 842–846.
[3] J.D. Jorgensen, J. Appl. Phys. 49 (1978) 5473–5478.

[4] B. Houser, N. Alberding, R. Ingalls, E.D. Corzier, Phys. Rev. B 37 (1988) 6513–6516.
[5] T. Yamanaka, K. Ogata, J. Appl. Crystallogr. 24 (1991) 111–118.
[6] M. Madon, P. Gillet, C. Julien, G.D. Price, Phys. Chem. Miner. 18 (1991) 7–18.
[7] J. Glinnemann, H.E. King Jr., H. Shulz, T. Hahn, S.J.L. Placa, F. Dacol, Z. Kristallogr. 198 (1992) 177–212.
[8] S. Kawasaki, O. Ohtaka, T. Yamanaka, Phys. Chem. Miner. 20 (1994) 531–535.
[9] T. Tsuchiya, T. Yamanaka, M. Matsui, Phys. Chem. Miner. 25 (1998) 94–100.
[10] E. Ghobadi, J.A. Capobianco, Phys. Chem. Chem. Phys. 2 (2000) 5761–5763.
[11] D.M. Christie, J.R. Chelikowsky, Phys. Rev. B 62 (2000) 14703–14711.
[12] C. Sevik, C. Bulutay, J. Mater. Sci. 42 (2007) 6555–6565.
[13] Q.J. Liu, Z.T. Liu, L.P. Feng, H. Tian, Solid State Sci. 12 (2010) 1748–1755.
[14] A.C. Camargo, J.A. Igualada, A. Beltran, R. Llusar, E. Longo, J. Andres, Chem. Phys. 212 (1996) 381–391.
[15] Z. Lodziana, K. Parlinski, J. Hafner, Phys. Rev. B 63 (2001) 134106.
[16] T. Tamura, G.H. Lu, R. Yamamoto, M. Kohyama, Phys. Rev. B 69 (2004) 195204.
[17] A.F. Zatsepin, V.S. Kortov, V.A. Pustovarov, D.Yu. Biryukov, Phys. Stat. Sol. C 2 (2005) 351–354.
[18] D.L. Griscom, Opt. Mater. Exp. 1 (2011) 400–412.
[19] A.N. Kislov, M.O. Toropov, A.F. Zatsepin, J. Non-Cryst. Solids 357 (2011) 1912–1915.
[20] R.W.G. Wyckoff, Crystal Structures, Wiley Interscience, New York, 1960.
[21] A.N. Kislov, V.G. Mazurenko, K.N. Korzov, V.S. Kortov, Physica B 352 (2004) 172–178.
[22] A.N. Kislov, Zinc oxide – a material for micro- and optoelectronic applications, in: N.H. Nickel, E. Terukov (Eds.), NATO Science Series, vol. 194, Kluwer Academic, Amsterdam, 2004.
[23] D.D. Richardson, Comput. Phys. Commun. 28 (1982) 75–101.
[24] B.W.H. van Beest, G.J. Kramer, R.A. van Santen, Phys. Rev. Lett. 64 (1990) 1955–1958.
[25] A.R. George, C.R.A. Catlow, J. Solid State Chem. 127 (1996) 137–144.
[26] R.D. Oeffner, S.R. Elliott, Phys. Rev. B 58 (1998) 14791–14803.
[27] P.E. Meek, Philos. Mag. 33 (1976) 897–908.
[28] C. Herscovici, M. Fibish, J. Phys. C.: Solid State Phys. 13 (1980) 1635–1647.
[29] K.V. Shanavas, N. Garg, S.M. Sharma, Phys. Rev. B 73 (2006) 094120.